

# An Information Theoretic Approach Characterizing Diffusion Anisotropy in Diffusion-weighted Magnetic Resonance Images

Nader S. Metwalli, Stephen M. LaConte, *Member, IEEE*, and Xiaoping P. Hu, *Senior Member, IEEE*

**Abstract**— We propose an alternative approach that does not rely on tensor models for characterizing diffusion anisotropy from diffusion-weighted magnetic resonance images. Information content inherent in the diffusion attenuation values are the only measures needed for our characterization. We explore the information content inherent in these values. We calculate Shannon's entropy on the diffusion attenuation values measured across the applied diffusion-sensitizing gradient directions. This method is evaluated with data generated with different diffusion gradient encoding schemes demonstrating the validity of our approach and its potential use to better differentiate between brain tissue types over tensor-based measures.

## I. INTRODUCTION

THE basis for diffusion tensor imaging (DTI) was introduced over a decade ago [1]. It attempts to characterize the random Brownian motion type diffusion observed in both isotropic and anisotropic media using a rank-2 tensor. DTI derived indices such as Fractional Anisotropy (FA) and Relative Anisotropy (RA) [2] are widely used. The underlying assumption in DTI is that the diffusion follows a Gaussian diffusion model. This assumption of a Gaussian diffusion profile is not always met, especially in cases of voxels having multiple fiber orientations [3]. In those situations, the tensor model is inadequate and this inadequacy propagates to the tensor derived anisotropy indices.

To circumvent this limitation we introduce an alternative approach for characterizing diffusion anisotropy directly from the diffusion-weighted magnetic resonance images. In communication theory, entropy reflects how uncertain we are of the outcome of a random variable thus making it a reasonable measure of information [4]. We apply Shannon's

Manuscript received April 24, 2006. This work was supported in part by NIH/NIDA grant (DA017795-01), NIH grant (RO1 EB002009), the Georgia Research Alliance, and the Whitaker Foundation.

N. S. Metwalli is a bioengineering Ph. D. student with the Wallace H. Coulter Department of Biomedical Engineering, Georgia Institute of Technology and Emory University, Atlanta, GA 30332 USA, a graduate research assistant with the Biomedical Imaging Technology Center (BITC), Georgia Institute of Technology and Emory University (e-mail: [nader.metwalli@bme.gatech.edu](mailto:nader.metwalli@bme.gatech.edu)) and a lecturer assistant in the Biomedical Engineering Dept., Faculty of Engineering, Cairo University, Cairo, Egypt.

S. M. LaConte, is with the Biomedical Imaging Technology Center (BITC), and an assistant professor with Emory University, Atlanta, GA 30322 USA (e-mail: [slaconte@bme.emory.edu](mailto:slaconte@bme.emory.edu)).

X. P. Hu is director of the Biomedical Imaging Technology Center (BITC), professor at the Wallace H. Coulter Department of Biomedical Engineering, Georgia Institute of Technology and Emory University, Atlanta, GA 30332 USA, and Georgia Research Alliance Eminent Scholar in Imaging (e-mail: [xhu@bme.emory.edu](mailto:xhu@bme.emory.edu)).

entropy to investigate the information content of the diffusion-weighted data. We estimate Shannon's entropy in the data measured with diffusion-sensitizing gradients in different directions on a per voxel basis. Shannon's entropy is a basic concept in information theory.

## II. METHODS

### A. Diffusion Imaging and Information Theory

Diffusion-weighted and DTI techniques are based on probing the random translational motion of water molecules that diffuse passively throughout the human body. Diffusion anisotropy is a direct consequence of biological barriers and hindrances the water molecules experience as they passively diffuse. The fundamental assumption is that these diffusing molecules probe, on a microscopic scale, the underlying tissue structure [5]. Diffusion-sensitizing gradients project the water molecule's diffusion profile in an underlying voxel along the direction of the applied gradient. The diffusion is observed as an attenuation in the magnetic resonance (MR) signal [5]. As a direct result of anisotropic diffusion profiles the measured attenuation values will vary and will depend directly on the shape of the diffusion profile and its projection along that direction.

Based on this, we hypothesized that tissue types with varying diffusion anisotropy profiles could be differentiated based on their underlying information content. We hypothesize that as diffusion anisotropy increases so does uncertainty reflected in Shannon's entropy [4]. Specifically entropy is calculated as,

$$H(X_i) = - \sum_{x_i \in K} p(x_i) \log p(x_i) \quad (1)$$

Where  $X_i$  is the attenuation of the MR signal due to water displacement along a certain spatial orientation.  $K$  is the set of all diffusion-sensitizing gradient directions, and  $p(x_i)$  is the probability of that attenuation value being repeated throughout  $K$ . The attenuation value for each voxel in each diffusion direction is calculated by dividing its diffusion-weighted signal intensity by that voxel's diffusion-free signal intensity.  $p(x_i)$  is calculated by binning the attenuation values for each voxel across the diffusion gradients and a histogram is constructed from which the  $p(x_i)$ 's are derived. The logarithm is to the base 2 casting the measured entropy or information to be expressed in binary digits or bits.

In communication theory, Shannon's entropy represents the average or mean amount of information per message

relayed through a communications channel [4]. Recent work [6], [7] derived generalized scalar measures based on entropy from tensors with rank higher than two, termed higher-rank diffusion tensors. Related work [8] applied directional entropy to the rank-2 diffusion tensor. In our approach we do not estimate any tensors.

Attenuation values resulting from water diffusing in a purely isotropic tissue as the cerebrospinal fluid (CSF) in the brain will not depend on the diffusion gradient direction along which diffusion is projected because the diffusion is isotropic. When these values are binned the histogram for CSF will be normally peaked, indicating that these values have a high probability of occurrence across all the diffusion directions. All remaining possible values will take on probabilities that are significantly smaller. Based on that, we expect  $H$  to be close to zero for CSF as  $H = 0$  if and only if all the  $p(x_i)$  but *one* are zero, with this one probability having the value of unity. Thus only when we are certain of the outcome does  $H$  vanish. Otherwise  $H$  is positive [4]. This, however, is not the case with tissue that is slightly anisotropic like brain gray matter (GM) or tissue that is highly anisotropic such as brain white matter (WM). For WM, which is a highly structured tissue, the attenuation values will strongly depend on the direction along which the diffusion gradient is applied. The histogram for the WM attenuation values will be more spread out across the bins. In this case, there definitely is information to be gained when the gradient directions are varied in space as demonstrated by histograms presented later.

#### B. Diffusion imaging measurements and analysis

We acquired diffusion-weighted images from 2 normal male volunteers (ages 18 and 26). The data was acquired on a Siemens 3.0T Trio with an imaging protocol employing a diffusion-weighted single-shot echo planar imaging sequence (courtesy Massachusetts General Hospital). Diffusion-weighted images for the first subject were acquired along 12 and 48 directions respectively. For the second subject, diffusion-weighted images were acquired along 60 directions. The data for both subjects was acquired with two  $b$ -values,  $1000 \text{ s/mm}^2$ , along with a single image acquired without diffusion weighting ( $b \approx 0$ ). The imaging parameters were as follows: TR = 8000 ms, TE (for 12 directions) = 100 ms, TE (for 48 directions) = 103 ms, TE (for 60 directions) = 104 ms, field of view (FOV) = 256 mm x 256 mm, matrix size of 128 x 128 with slice thickness 2 mm giving an overall isotropic resolution of 2 mm x 2 mm x 2 mm, phase partial Fourier of 6/8 and number of averages = 1 for the 12 and 48 directions. For the second subject, we acquired the same volume 3 times with the 60 diffusion directions for subsequent averaging. Each separate scan took  $\sim 7$  minutes.

#### C. Entropy and DTI analysis

The acquired diffusion-weighted data was first skull-stripped using BET [9] and then corrected for eddy currents and head motion using an affine registration to a reference

volume, the diffusion-free image [10].

The diffusion-weighted images of each slice were normalized by dividing them by the diffusion-free images on a voxel-by-voxel basis. The entropy of each voxel was calculated using (1). All entropy analysis was done in Matlab (Mathworks, Inc., Natick, Massachusetts). The diffusion tensor for each voxel was estimated using FDT [11]. When the tensors are diagonalized the principal diffusion directions, eigenvectors, along with the principal diffusivity values, eigenvalues, are produced. The fractional anisotropy (FA) map which employs the resulting eigenvalues from the diagonalization was also produced through FDT. FA values range from zero corresponding to complete isotropy to unity indicating infinite anisotropy. WM takes on values close to one appearing whiter in FA map images than both GM and CSF, the latter appearing the darkest.

### III. RESULTS

#### A. Entropy and DTI data

The results of our entropy and DTI analysis are shown in Figs. 1A, 1B, 2A, and 2B, for a selected slice. The 12 direction diffusion data is not shown because of its poor signal-to-noise ratio attributed to the decreased number of directions and that the data was acquired with one average. Figs. 1A and 1B are 48 diffusion direction data from the first

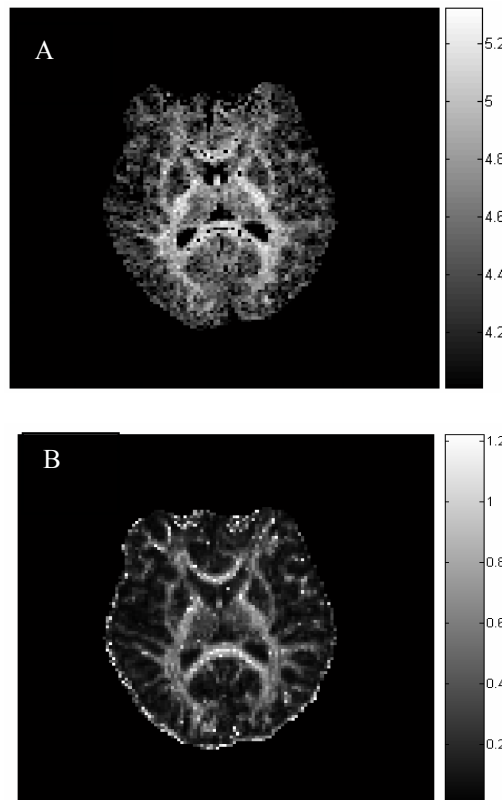


Fig. 1. 48 diffusion direction data. (A) Entropy map (B) Fractional anisotropy (FA) map. Corresponding major white matter (WM) structures are clearly visible in both A and B.

subject. Figs. 1A and 2A are the entropy analysis and Figs.

1B and 2B are the fractional anisotropy maps generated in FSL (<http://www.fmrib.ox.ac.uk/fsl/>). The decreased quality of the images in Fig. 1 is due to the fact that they were acquired with one average. Figs. 2A and 2B display 60 diffusion direction data (averaged from 3 measurements) for the second subject. The location of the slice was chosen to closely match the location of the images for the first subject.

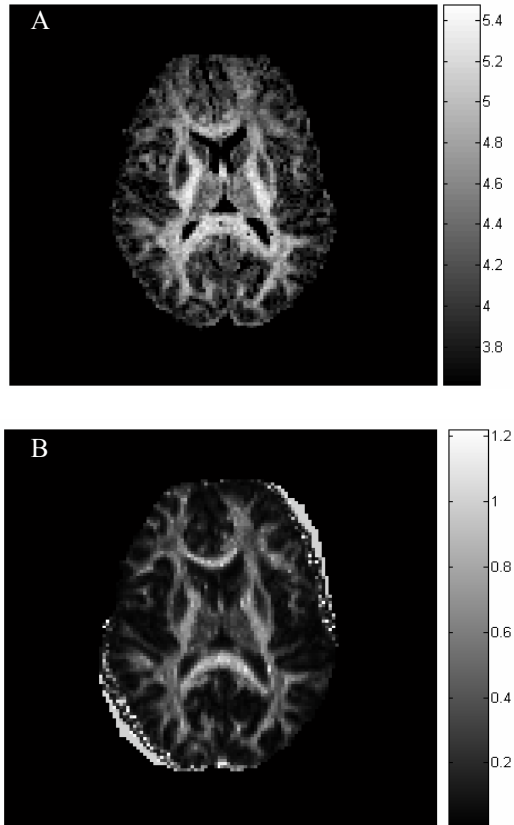


Fig. 2. 60 diffusion direction data. (A) Entropy map (B) Fractional anisotropy (FA) map. We point out here that the thalamus is more visible in the entropy image than the FA map in Fig. 2B. Gray matter (GM) and cerebrospinal fluid (CSF) can be distinguished on the entropy map however the same can not be said for the FA map.

As we hypothesized, tissues with different diffusion anisotropy display differing ranges of entropy. From our results higher anisotropy in a tissue is reflected as having higher information content. This higher information content is reflected as higher entropy (i.e. an increase in the average number of bits needed to represent the tissue). Using more diffusion gradient directions in the acquisition scheme improved the entropy estimation and enhanced the anisotropy-dependent contrast as shown in our data.

Figs. 3, 4, and 5 represent histograms for representative CSF, GM, and WM voxels, respectively, in the slice presented in Fig. 2. In Fig. 3 the CSF attenuation values are clustered closely together at the left end of the histogram. This leads to these attenuation values taking on a substantially higher probability of occurring over the rest of the values in the histogram. Therefore as we expected,  $H$  is close to zero.

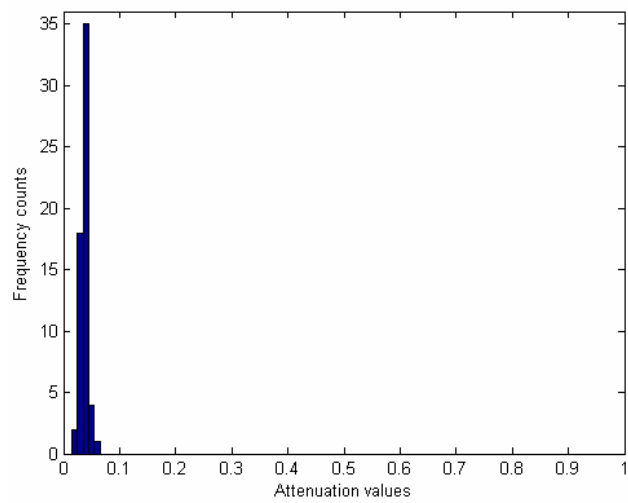


Fig. 3. Histogram of representative cerebrospinal fluid (CSF) voxel attenuation values. Note the dense clustering of attenuation values at the left tail of the histogram.

In Figs. 4 and 5, we notice that the histograms of both GM and WM are more dispersed leading to entropy being higher than that of the CSF. Furthermore, the WM histogram is broader than GM accounting for the higher entropy in the WM.

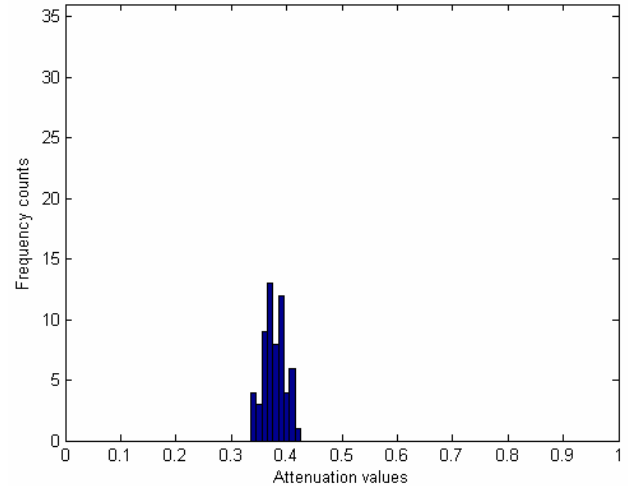


Fig. 4. Histogram of representative gray matter (GM) voxel attenuation values.

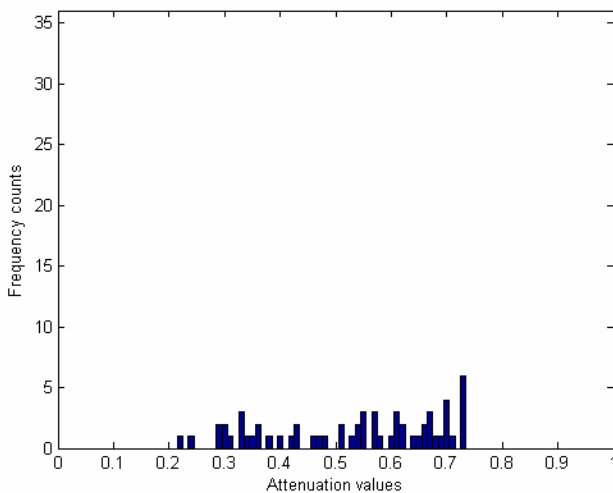


Fig. 5. Histogram of representative white matter (WM) voxel attenuation values. Note how the values are more dispersed along the histogram as contrasted with CSF voxel attenuation values in Fig. 3.

The difference in entropy values between various tissue types (CSF, GM, and WM) is a direct result of their different histograms. To verify this, average entropy values were calculated for three regions-of-interest (ROIs) in CSF, GM, and WM. The ROIs are depicted in Fig. 6 and the results are shown in Table 1.

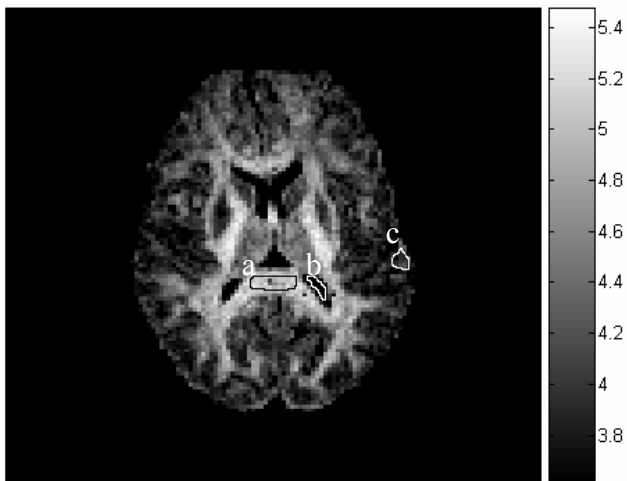


Fig. 6. Regions-of-interest (ROIs) taken in white matter (WM), gray matter (GM) and cerebrospinal fluid (CSF). The WM ROI (a) is outlined in black and those for the CSF (b) and GM (c) are marked with white.

TABLE I  
ENTROPY AVERAGES IN THE DIFFERENT TISSUE TYPES

Tissue type in ROI	Mean (std)
CSF	2.7 (0.12)
GM	3.9 (0.18)
WM	5.1 (0.13)

The standard deviation of the entropy (std) is shown in parentheses.

#### IV. CONCLUSIONS

We have introduced and demonstrated an entropy measure for characterizing diffusion anisotropy. This method assumes no underlying model from which indices characterizing diffusion anisotropy are derived, but extracts the diffusion anisotropy directly from the data. The measure seems to provide additional contrast between different tissues and may reveal anisotropy that is missed by tensor-based measures.

#### ACKNOWLEDGMENT

The authors would like to thank Richard Cameron Craddock and Jeff Prescott for helpful discussions.

#### REFERENCES

- [1] P. J. Basser, J. Mattiello, and D. LeBihan, "Estimation of the Effective Self-Diffusion Tensor from the NMR Spin Echo," *Journal of Magn. Reson.*, Series B 103, pp. 247-254, 1994.
- [2] C. Pierpaoli and P. J. Basser, "Toward a Quantitative Assessment of Diffusion Anisotropy," *Magn. Reson. Med.*, 36, pp. 893-906, 1996.
- [3] D. S. Tuch, *et al.*, "High Angular Resolution Diffusion Imaging Reveals Intravoxel White Matter Fiber Heterogeneity," *Magn. Reson. Med.*, 48, pp. 577-582, 2002.
- [4] C. E. Shannon, "A Mathematical Theory of Communication," *The Bell Sys. Tech. Jour.*, 27, pp. 379-423, 623-656, July, October, 1948.
- [5] D. Le Bihan, *et al.*, "Diffusion Tensor Imaging: Concepts and Applications," *Journal of Magn. Reson. Img.*, 13, pp. 534-546, 2001.
- [6] E. Ozarslan, and T. H. Mareci, "Anisotropy as a Certainty Measure in terms of Entropy," in *Proc. Intl. Soc. Mag. Reson. Med.*, Toronto, 2003, pp. 249.
- [7] E. Ozarslan, B. C. Vemuri and T. H. Mareci, "Generalized Scalar Measures for Diffusion MRI Using Trace, Variance, and Entropy," *Magn. Reson. Med.*, 53, pp. 866-876, 2005.
- [8] T. Neuvonen and E. Salli, "Characterizing diffusion tensor imaging data with directional entropy," in *Proc. 2005 IEEE Engineer. Med. Biol. 27<sup>th</sup> Annu. Conf.*, Shanghai, 2003, pp. 5798-5801.
- [9] S. M. Smith, "Fast Robust Automated Brain Extraction" *Human Brain Mapp.*, 17(3), pp. 143-155, 2002.
- [10] M. Jenkinson and S. M. Smith, "A Global Optimization Method for Robust Affine registration of Brain Images," *Med. Image Anal.*, 5(2), pp. 143-156, 2001.
- [11] T. E. J. Behrens, *et al.*, "Characterization and Propagation of Uncertainty in Diffusion-Weighted MR Imaging," *Magn. Reson. Med.*, 50(5), pp. 1077-1088, 2003.